EPJ manuscript No.
(will be inserted by the editor)

Relativistic transition wavelenghts and probabilities for spectral lines of Ne II

J. P. Santos[1a], A. M. Costa[2], C. Madruga[1], F. Parente[1], and P. Indelicato[3]

[1] Centro de Física Atómica, Departamento de Física, Faculdade de Ciências e Tecnologia, FCT, Universidade Nova de Lisboa, Monte de Caparica, 2829-516 Caparica, Portugal
[2] Centro de Física Atómica, Departamento de Física, Faculdade de Ciências, FCUL, Universidade de Lisboa, Campo Grande, Ed. C8, 1749-016 Lisboa, Portugal
[3] Laboratoire Kastler Brossel, École Normale Supérieure, CNRS, Université P. et M. Curie – Paris 6, Case 74; 4, place Jussieu, 75252 Paris CEDEX 05, France

January 19, 2013

Abstract. Transition wavelengths and probabilities for several $2p^4$ 3p - $2p^4$ 3s and $2p^4$ 3d - $2p^4$ 3p lines in fluorine-like neon ion (NeII) have been calculated within the multiconfiguration Dirac-Fock (MCDF) method with quantum electrodynamics (QED) corrections. The results are compared with all existing experimental and theoretical data.

PACS. 3 1.15.vj Electron correlation calculations for atoms and ions: excited states, 32.70.Cs Oscillator strengths, lifetimes, transition moments, 32.30.Jc Visible and ultraviolet spectra

1 Introduction

Knowledge of accurate atomic parameters, such as transition probabilities, is fundamental in the study of atomic structure, and of laboratory or astrophysical plasmas. In what concerns astrophysics, these parameters are crucial to estimate the densities of species in the atmospheres of stars, galaxies and nebulae [1].

Neon, after H, He, O, and C, is one of the most abundant elements in Universe and is one of the products of hydrogen and helium thermonuclear reactions in the orderly evolution of stellar interiors [2].

Because of its cosmic abundance and atomic properties all neon ions are of importance in various astrophysical sources, in particular Ne II, whose emission lines are very intense.

The interest in the spectrum of Ne II has been further stimulated by large discrepancies between the existing transition probability values of the spontaneous emission rates (Einstein's A_{ki} values) for weak intercombination, or spin-forbidden, lines.

Koopman [3] performed the first extensive measurements of Ne II spectra, covering around 50 lines, using an electrically driven shock tube as the spectroscopic source and adjusted in some cases with the help of the J-file sum rule proposed by Condon an Shortley [4]. This rule, used in systems that do not accurately follow the LS coupling scheme, relates the sum of the oscillator strengths of the lines with a common upper or lower level to the quantum weight of that state. Koopman's work is one of the original references given in the NIST-ASD compilation [5].

Extensive spontaneous-emission data on Ne II using a water-cooled neon-ion-laser discharge without any mirrors as the spectroscopic source were obtained by [6].

After more than twenty years since the last reported measured values, Burshtein and Vujnovic [7] obtained the absolute transition probabilities of the 3p-3s transition array within an overall uncertainty of 25%.

Griesman *et al.* [8], using a high-current hollow-cathode lamp, provided absolute measurements of transition probabilities for 48 Ne II lines, and relative measurements for 83 Ne II lines, corresponding to 3p, 3d and 4s upper levels and including many weak intersystem lines for the first time. Their uncertainty is 11% for strong lines ($A_{ki} > 0.1 \times 10^8$ s^{-1}), increasing to 32% for weaker lines.

In 1999, Fuhr and Wiese [9] published a critical compilation of atomic transition probabilities for about 9000 selected lines of all elements, mainly for neutral and singly ionized spectra, to which they assigned an uncertainty band of 25-50%.

Using a pulsed discharge lamp emission experiment, Val *et al.* [10] reported transition probability values for 94 Ne II lines, in the 337-463 nm spectral region. Their absolute A_{ki} values were obtained by using bibliographic data as reference and, consequently, their quality is linked to the intrinsic quality of these data. They estimated an average error around 15% for A_{ki} transition values larger than 0.2×10^8 s^{-1} and around 30% for the weakest transitions.

Send offprint requests to: J. P. Santos
[a] jps@fct.unl.pt

Djenize *et al.* [11] measured the transition probabilities of 42 Ne II spectral lines in a linear low-pressure pulsed arc. The transition probabilities were obtained using the relative line intensity ratio method. Their uncertainties range from 10% to 20%.

Using a high-current hollow cathode discharge in pure neon Bridges and Wiese [12] studied experimentally weak intersystem lines and related strong persistent lines of Ne II. They obtained transition probabilities for some 3p-3s, 3d-3p and 4f-3d lines with uncertainties smaller than 25%, 27% and 31%, respectively.

In what concerns the theoretical work, Garstang [13] performed, to our knowledge, the first Ne II ion transition probability calculations using the intermediate coupling approximation and parameters determined empirically from observational data.

Marantz [14] calculated, within the intermediate coupling approximation, the radial wavefunctions by using the computer program developed by Herman and Skillman [15], and obtained results very similar to those given by Garstang.

Using the general configuration interaction code CIV3, Blackford and Hibbert [16] reported calculations for transitions in F-like ions in the range $Z = 10, \ldots, 33$. Only a limited amount of correlation was included within the $n = 2$ electrons, and the Breit-Pauli Hamiltonian included only the mass correction, Darwin terms, and a one-electron spin-orbit operator. These authors have made some adjustments to the transition energies to bring them close to experimental energy separations.

Froese Fischer and He [17] performed calculations for some Ne II transitions taking two approaches: the multiconfiguration Hartree-Fock (MCHF) method with Breit-Pauli corrections, omitting only the orbit-orbit term, which does not contribute to term mixing, and the multiconfiguration Dirac-Hartree-Fock (MCDHF) method with Breit correction. The latter method allowed the authors to compute the results in two different gauges: in the Coulomb (velocity) gauge and Babushkin (length) gauge.

Godefroid and Hibbert [18] re-analyzed some CIV3 results for Ne II and found that the major reason for the discrepancy with the earlier MCHF data by Froese Fischer and He [17] was mainly related to the omission of the "fine-tuning" in the previous calculations, which is made by correcting empirically the off-diagonal coupling Hamiltonian matrix element, assuming a proportionality between the coupling term and the fine-structure energy separation.

Zheng and Wang [19] employed the Weakest Bound Electron Potential Model (WBEPM) method to calculate some transition probabilities for individual lines of Ne II. The needed parameters for this method were determined by fitting the experimental value of energy level and the expectation value of radial distance.

Recently, Froese Fischer and Tachiev [20] reported energy levels, lifetimes, and transition probabilities for, among others, the F-like ($Z = 9, \ldots, 14$) sequence. The wavefunctions were determined using the MCHF method with relativistic effects included through the Breit-Pauli Hamiltonian, omitting only the orbit-orbit interaction. Afterwards, the calculated transition probabilities were "adjusted" by correcting the transition energy using the available experimental data. The authors reported that the shifts in the energy adjustments were considerably smaller than in the earlier MCHF calculations for Ne II [17] due to the inclusion of more correlation, and concluded that the MCDHF levels published in reference [17] were not correctly ordered.

In the present *ab initio* theoretical work we start from a Dirac-Fock calculation with Breit interaction included self-consistently. Higher-order retardation and one-electron radiative corrections are also included, and the screening of the self-energy is evaluated using the Welton approximation. Correlation is added within the multiconfiguration Dirac-Fock method (MCDF). In this framework we have calculated the relativistic transition wavelengths for several Ne II $2p^4$ 3p - $2p^4$ 3s and $2p^4$ 3d - $2p^4$ 3p lines, and used them to compute the transition probabilities.

2 Relativistic calculations

Ne II has seven electrons outside the $1s^2$ core, which produce interactions in the excited states. In order to obtain accurate results in an *ab initio* based in the Configuration Interaction (CI) method, a large number of configurations should be considered to deal with these interactions, making the calculation very complex and time consuming. Another problem of this *ab initio* method is to select a proper configuration wave function, especially for excited states, because different selections of configuration wave function make accuracy of different results.

The MCDF approach, being a variational method, has the advantage of providing, with smaller basis sets, results of the same accuracy of those obtained with the CI method, or variants.

The general relativistic program developed by Desclaux and Indelicato [21,22,23] was used to compute the energies and wavefuntions, as well as radiative transition probabilities within the MCDF method.

In order to obtain a correct relationship between many-body methods and quantum electrodynamics (QED), one should start from the no-pair Hamiltonian [24,25,26,27]

$$\mathcal{H}^{\text{no pair}} = \sum_{i=1}^{N} \mathcal{H}_D(r_i) + \sum_{i<j} \mathcal{V}(|\boldsymbol{r}_i - \boldsymbol{r}_j|), \qquad (1)$$

where $\mathcal{H}_D$ is the one electron Dirac operator and $\mathcal{V}$ is an operator representing the electron-electron interaction of order one in α, properly set up between projection operators $\Lambda_{ij}^{++} = \Lambda_i^+ \Lambda_j^+$ to avoid coupling positive and negative energy states

$$\mathcal{V}_{ij} = \Lambda_{ij}^{++} V_{ij} \Lambda_{ij}^{++}. \qquad (2)$$

The expression of V_{ij} in the Coulomb gauge and in atomic units is

$$V_{ij} = \frac{1}{r_{ij}} \quad (3)$$

$$-\frac{\boldsymbol{\alpha}_i \cdot \boldsymbol{\alpha}_j}{r_{ij}} \quad (4)$$

$$-\frac{\boldsymbol{\alpha}_i \cdot \boldsymbol{\alpha}_j}{r_{ij}}\left[\cos\left(\frac{\omega_{ij} r_{ij}}{c}\right) - 1\right]$$

$$+c^2(\boldsymbol{\alpha}_i \cdot \boldsymbol{\nabla}_i)(\boldsymbol{\alpha}_j \cdot \boldsymbol{\nabla}_j)\frac{\cos\left(\frac{\omega_{ij} r_{ij}}{c}\right)-1}{\omega_{ij}^2 r_{ij}}, \quad (5)$$

where $r_{ij} = |\boldsymbol{r}_i - \boldsymbol{r}_j|$ is the inter-electronic distance, ω_{ij} is the energy of the exchanged photon between the two electrons, $\boldsymbol{\alpha}_i$ are the Dirac matrices and c is the speed of light [28].

The term (3) represents the Coulomb interaction, the term (4) is the Gaunt (magnetic) interaction, and the last two terms (5) stand for the retardation operator. In this expression the $\boldsymbol{\nabla}$ operators act only on r_{ij} and not on the following wave functions.

By a series expansion of the operators in expressions (4) and (5) in powers of $\omega_{ij} r_{ij}/c \ll 1$ one obtains the Breit interaction, which includes the leading retardation contribution of order $1/c^2$. The Breit interaction is, then, the sum of the Gaunt interaction (4) and the Breit retardation

$$B_{ij}^{\mathrm{R}} = \frac{\boldsymbol{\alpha}_i \cdot \boldsymbol{\alpha}_j}{2r_{ij}} - \frac{(\boldsymbol{\alpha}_i \cdot \boldsymbol{r}_{ij})\,(\boldsymbol{\alpha}_j \cdot \boldsymbol{r}_{ij})}{2r_{ij}^3}. \quad (6)$$

In the many-body part of the calculation the electron-electron interaction is described by the sum of the Coulomb and the Breit interactions. Higher orders in $1/c$, deriving from the difference between Eqs. (5) and (6) are treated here only as a first order perturbation.

All calculations are done for a finite nucleus using a uniformly charged sphere. The atomic mass and the nuclear radius were taken from the tables by Audi *et al.* [29] and Angeli and [30], respectively.

Radiative corrections are also introduced, from a full QED treatment. The one-electron self-energy is evaluated using the one-electron values of Mohr and co-workers [31, 32,33,34] and corrected for finite nuclear size [35].

The self-energy screening and vacuum polarization are treated with an approximate method developed by Indelicato and co-workers [36,37,38,39,40].

For each transition, initial and final states are computed independently to get accurate correlation energies. Consequently, the initial and final state orbitals of identical symmetry are not orthogonal (see, e.g. [41] and references therein). This non-orthogonality is properly taken in account in the transition probability calculation using Löwdin's method [42]. Being a fully relativistic method, initial and final levels for each transition are defined in jj-coupling. However, for comparison with other published work where levels are characterized by their LSJ values, we show in the tables, for each level, the most important LSJ set of values which results from the expansion of the jjJ wave function in terms of LSJ ones.

3 Results and discussion

When the wave functions are determined variationally, the energy of a particular atomic level will be the lowest that can be achieved with the specific form used for the wave function. Improvements in the wave function, such as the inclusion of more configuration state functions to account for electronic correlation, will lead, in principle, to monotonic reductions in the energy, which guarantees the improvement of the energy accuracy.

Unlike in the evaluation of energies, there is no guaranteed monotonic improvement in the energy separations between atomic levels (transition energy) with respect to improvements in the wave function. Nevertheless, this problem can be overcome by optimizing, in a systematic manner, both the wave function and energy of each level, so that the two states are treated, as far as possible, in a balanced way. Consequently, the amount of correlation included in the calculation of the wave function and energy must be equivalent for both initial and final levels.

The results obtained in this work for the $1s^2\ 2s^2\ 2p^4\ 3p\ {}^4P_{7/2}-1s^2\ 2s^2\ 2p^4\ 3s$ transition wavelength, shown in Table 1, are an example of the importance of the inclusion of correlation. We observe that the calculated single-configuration Dirac-Fock wavelength differs by about 4% from the experimental value. The inclusion of correlation narrows this difference to less than 0.3%. It is worthwhile to call attention to the fact that the correlation configuration $2p^2\ 3p\ 6\ell^2$, in the upper level, and the $2p^2\ 3s\ 6\ell^2$ one in the lower level, with ℓ =s...f, give only a contribution of 0.25 nm to the wavelength, which is 0.08% of the calculated value. Furthermore, we observe that the inclusion of the mentioned configurations with ℓ =f gives no contribution to the wavelength value.

Considering this analysis, to obtain the valence and the core-valence correlation contributions we used a virtual space spanned by single and double-excited configurations up to 3d orbitals, resulting from the excitation of $n = 2$ and $n = 3$ electrons in the upper and lower levels, and the double-excited configurations $2p^2\ 3p\ n'\ell^2$, for the upper level, and $2p^2\ 3s\ n'\ell^2$, with $n'\ell^2$ =$4s^2$...$6d^2$. This educated choice allowed us to maintain a manageable virtual orbital space, and to avoid the nonrelativistic offset through the inclusion of the "Brillouin" single excitations [44].

A comparison between the results of this work for the transition wavelengths and Kramida and Nave's experimental results [43], published in the NIST webpage [5], is presented in Tables 2 and 3, and illustrated in Figure 1. We observe that all theoretical results differ by less than 6% from the experimental ones, and more than 20% differ by less than 1% from the Kramida and Nave's results. This agreement validates our transition wavelength results.

The role of gauge invariance in the interaction between the electromagnetic field and the electron-positron field is discussed explicitly in well-known texts [45]. Existing relativistic self-consistent-field calculations of radiative atomic transition probabilities have been carried out in the Coulomb or Babushkin gauges. In the nonrelativistic limit the Coulomb gauge formula for the transition

Table 1. Correlation effect on $1s^2\ 2s^2\ 2p^4\ 3p\ {}^4D_{7/2} \rightarrow 1s^2\ 2s^2\ 2p^4\ 3s\ {}^4P_{5/2}$ transition wavelength λ (in nm) and transition probability A_{ki} (in 10^8 s^{-1}). The $1s^2\ 2s^2$ core is omitted in the table entries.

Upper level ($^4D_{7/2}$)	Lower level ($^4P_{5/2}$)	λ	$A_{ki,\mathrm{length}}$	$A_{ki,\mathrm{velocity}}$
$2p^4\ 3p$	$2p^4\ 3s$	347.26	1.733	1.659
+ All correlation until 3d	+ All correlation until 3d	319.51	2.139	1.895
+ $2p^2\ 3p\ 4s^2$ + $2p^2\ 3p\ 4p^2$	+ $2p^2\ 3s\ 4s^2$ + $2p^2\ 3s\ 4p^2$	332.57	1.905	1.832
+ $2p^2\ 3p\ 4d^2$ + $2p^2\ 3p\ 4f^2$	+ $2p^2\ 3s\ 4d^2$ + $2p^2\ 3s\ 4f^2$	333.03	1.897	1.829
+ $2p^2\ 3p\ 5s^2$ + $2p^2\ 3p\ 5p^2$	+ $2p^2\ 3s\ 5s^2$ + $2p^2\ 3s\ 5p^2$	333.85	1.883	1.825
+ $2p^2\ 3p\ 5d^2$ + $2p^2\ 3p\ 5f^2$	+ $2p^2\ 3s\ 5d^2$ + $2p^2\ 3s\ 5f^2$			
+ $2p^2\ 3p\ 5g^2$	+ $2p^2\ 3s\ 5g^2$	333.94	1.882	1.824
+ $2p^2\ 3p\ 6s^2$ + $2p^2\ 3p\ 6p^2$	+ $2p^2\ 3s\ 6s^2$ + $2p^2\ 3s\ 6p^2$	334.06	1.880	1.824
+ $2p^2\ 3p\ 6d^2$	+ $2p^2\ 3s\ 6d^2$	334.23	1.878	1.814
+ $2p^2\ 3p\ 6f^2$	+ $2p^2\ 3s\ 6f^2$	334.23	1.878	1.814
Experimental		333.48[§]	1.77±0.15 [†]	

[§] Ref. [43].
[†] $A_{\mathrm{Exp_{Av}}}$.

probability yields the dipole velocity expression whilst the Babushkin formula gives the dipole length expression [46].

From the point of view of the transition probability accuracy, an important requisite is the agreement between length and velocity forms. Nevertheless, one should be cautious about drawing conclusions from such an agreement in the relativistic case, since it depends on the proper inclusion of the negative energy state [47], which cannot be explicitly done in the present calculations. When there is no good agreement between the two forms, there are reasons for a preference of the length form over the velocity form from the non-relativistic [48,49] and relativistic [50] points of view.

A graphical comparison of our results with experimental results for the transition probabilities of the 3p-3s and 3d-3p is shown in Fig. 2 and 3, respectively. The line identification is given in Tables 2 and 3. The first conclusion we draw from these figures is that there is a large disagreement between the experimental results. The maximum relative difference between the experimental values for each transition spans a range from 45% to 200% in the 3p-3s transitions, and from 5% to 277% in the 3d-3p transitions. The average of these maxima is 45% for the former transitions and 71% for the latter ones. The cause of these discrepancies, even within experiments of the same type is puzzling. Possible reasons are misidentifications of the lines, normalization problems, and nonselective excitation of atomic energy levels.

In order to have an experimental reference to assess the theoretical calculations we computed, for each transition, the weighted average, $A_{\mathrm{Exp_{Av}}}$, using as weight, for each case, the inverse of the square of the uncertainty.

In the cases the uncertainty is not provided, such as Koopman [3], Hodges and Marantz [6], Burshtein and Vujnovic [7], and Fuhr and Wiese [9], we have assumed an uncertainty of 30%.

In Tables 2 and 3, the transition probability values (A_{ki}) calculated in this work for several (^{3} P)3p – (^{3} P)3s and (^{3} P)3d – (^{3} P)3p lines (LS dipole-allowed and intersystem lines), respectively, in Ne II are compared with the available theoretical values of Garstang [13], Marantz [14], Blackford and Hibbert [16], Zheng [19], and Fischer and Tachiev [20], and with the experimental weighted average (EWA), $A_{\mathrm{Exp_{Av}}}$.

A general agreement between length and velocity forms of the transition probabilities is found; in 91% of our results the length and velocity forms of the oscillator strengths differ by less than 20% and in 60% of our results the two forms differ by less than10%.

Comparing our ab initio values and the adjusted results by Fischer and Tachiev [20] to the EWA values, in 50% of the 3d-3p lines our ab initio values are closer than the later adjusted values, and in 80% of the 3p-3s lines the adjusted Fischer and Tachiev values are closer than our values. In order to assess the influence of the inclusion of the experimental transition energies in the adjusted A_{ki} values, we present in Table 4, for some lines, the relative differences between our ab initio values $A_{\mathrm{TW,l}}$, our adjusted values with the NIST transition energies $A_{\mathrm{TW,l\ adjusted}}$, the adjusted Fischer and Tachiev values, and the weighted average experimental values $A_{\mathrm{Exp_{Av}}}$. We observe that in all analyzed cases the energy adjustment bring our ab initio results closer to the EWA values than the Fischer and Tachiev results. Nevertheless, we must emphasize that this agreement is only indicative, and should not be considered in an absolute way since, as mentioned earlier, there is a large disagreement between the experimental results and, consequently, the EWA reflect only an experimental trend.

Table 2. Wavelengths λ (in nm) and transition probabilities A_{ki} (in 10^8 s^{-1}) for some $3p-3s$ lines and comparisons with other theoretical and experimental results. $\lambda_{\rm TW}$, $A_{\rm TW,l}$ and $A_{\rm TW,v}$ represent, respectively, the wavelength and the transition probability values in the length and velocity gauges calculated in this work. $A_{\rm G}$, $A_{\rm M}$, $A_{\rm BH}$, $A_{\rm Z}$ and $A_{\rm FT}$ denote theoretical values taken from Garstang [13], Marantz [14], Blackford and Hibbert [16], Zheng [19], and Fischer and Tachiev [20], respectively. $\lambda_{\rm NIST}$ represent the experimental NIST values by Kramida and Nave [43], and $A_{\rm Exp_{Av}}$ the weighted average experimental values.

#	Upper level (k)	Lower level (i)	$\lambda_{\rm TW}$	$\lambda_{\rm NIST}$	$A_{\rm TW,l}$	$A_{\rm TW,v}$	$A_{\rm G}$	$A_{\rm M}$	$A_{\rm BH}$	$A_{\rm Z}$	$A_{\rm FT}$	$A_{\rm Exp_{Av}}$
	$(^3P)3p-(^3P)3s$											
1	$^2S_{1/2}$	$^2P_{1/2}$	356.57	355.78	0.29	0.27	0.75	0.22	0.44	···	0.22	0.22±0.01
2		$^2P_{3/2}$	349.62	348.19	1.53	1.31	0.77	1.44	1.19	1.13	1.39	1.45±0.08
3	$^2P_{1/2}$	$^2P_{1/2}$	325.46	337.82	1.54	1.70	0.85	1.52	1.19	1.25	1.48	1.49±0.09
4		$^2P_{3/2}$	324.75	330.97	0.50	0.55	0.94	0.22	0.51	···	0.26	0.24±0.02
5	$^2P_{3/2}$	$^2P_{1/2}$	326.39	339.28	0.44	0.47	0.40	0.39	0.32	0.31	0.39	0.38±0.02
6		$^2P_{3/2}$	325.68	332.37	1.63	1.81	1.35	1.42	1.42	1.62	1.38	1.40±0.08
7	$^2D_{3/2}$	$^2P_{1/2}$	372.43	372.71	1.18	1.12	0.98	1.07	1.10	1.16	1.06	0.93±0.05
8		$^2P_{3/2}$	365.51	364.39	0.34	0.30	0.33	0.33	0.30	0.25	0.33	0.36±0.02
9	$^2D_{5/2}$	$^2P_{3/2}$	384.63	371.31	1.30	1.32	1.29	1.38	1.41	1.40	1.37	1.14±0.06
10	$^4S_{3/2}$	$^4P_{1/2}$	306.92	302.89	0.52	0.46	0.32	0.51	0.55	0.40	0.45	0.43±0.03
11		$^4P_{3/2}$	304.66	300.17	0.91	0.78	0.76	0.92	0.90	0.81	0.84	0.75±0.05
12		$^4P_{5/2}$	299.21	295.57	1.16	0.96	1.40	1.25	1.13	1.27	1.12	0.96±0.06
13	$^4P_{1/2}$	$^4P_{1/2}$	363.97	375.12	0.20	0.23	0.18	0.19	0.19	0.21	0.18	0.17±0.01
14		$^4P_{3/2}$	377.62	370.96	1.09	1.22	1.10	1.20	1.23	1.07	1.14	1.04±0.05
15	$^4P_{3/2}$	$^4P_{1/2}$	365.99	377.71	0.47	0.53	0.47	0.44	0.86	0.51	0.42	0.35±0.02
16		$^4P_{3/2}$	362.79	373.49	0.23	0.25	0.20	0.20	0.19	0.17	0.19	0.16±0.01
17		$^4P_{3/2}$	359.94	366.41	0.81	0.82	0.45	0.75	0.80	0.60	0.71	0.62±0.03
18	$^4P_{5/2}$	$^4P_{3/2}$	365.98	376.63	0.31	0.35	0.29	0.31	0.31	0.37	0.30	0.27±0.01
19		$^4P_{5/2}$	375.24	369.42	1.01	1.11	1.02	1.08	1.11	0.90	1.03	0.90±0.04
20	$^4D_{1/2}$	$^4P_{1/2}$	339.23	334.44	1.61	1.39	1.54	1.64	1.67	1.48	1.53	1.41±0.21
21		$^4P_{3/2}$	334.31	331.13	0.23	0.22	···	0.27	0.28	0.30	0.26	0.27±0.05
22	$^4D_{3/2}$	$^4P_{1/2}$	336.20	336.06	0.91	0.84	0.84	0.87	0.88	0.73	0.82	0.84±0.07
23		$^4P_{3/2}$	333.49	332.72	0.94	0.84	0.89	0.97	1.00	0.96	0.91	0.90±0.07
24		$^4P_{5/2}$	327.68	327.08	0.05	0.04	0.06	0.06	0.06	0.09	0.06	0.05±0.008
25	$^4D_{5/2}$	$^2P_{3/2}$	389.36	394.23	0.01	0.01	0.01	0.01	0.003	···	0.01	0.01±0.002
26		$^4P_{3/2}$	335.67	335.50	1.47	1.35	1.35	1.43	1.47	1.23	1.34	1.27±0.19
27		$^4P_{5/2}$	329.78	329.77	0.42	0.37	0.42	0.46	0.46	0.55	0.47	0.42±0.06
28	$^4D_{7/2}$	$^4P_{5/2}$	334.23	333.48	1.88	1.81	1.81	1.92	1.95	1.77	1.80	1.77±0.15
	$(^1D)3p-(^1D)3s$											
29	$^2P_{3/2}$	$^2D_{3/2}$	324.22	334.58	0.23	0.27	0.17	0.25	0.05	···	0.23	0.18±0.04
30		$^2D_{5/2}$	324.18	334.55	1.79	2.17	1.50	1.53	1.75	···	1.47	1.33±0.28
31	$^2F_{5/2}$	$^2D_{3/2}$	356.97	357.46	1.49	1.42	1.30	1.44	1.51	···	1.40	1.23±0.08
32		$^2D_{5/2}$	356.94	357.42	0.13	0.11	0.09	0.11	0.11	···	0.11	0.10±0.01
33	$^2F_{7/2}$	$^2D_{5/2}$	350.86	356.85	1.68	1.53	1.30	1.57	1.63	···	1.51	1.29±0.09

Table 3. Wavelengths λ (in nm) and transition probabilities A_{ki} (in 10^8 s^{-1}) for some $3d-3p$ lines and comparisons with other theoretical and experimental results. $\lambda_{\rm TW}$, $A_{\rm TW,l}$ and $A_{\rm TW,v}$ represent, respectively, the wavelength and the transition probability values in the length and velocity gauges calculated in this work. $A_{\rm G}$, $A_{\rm M}$, $A_{\rm BH}$, $A_{\rm FH}$, $A_{\rm GF}$, $A_{\rm Z}$, $A_{\rm FT}$ denote theoretical values taken from Garstang [13], Marantz [14], Blackford and Hibbert [16], Fischer and He [17], Godefroid and Fischer [18], Zheng [19], and Fischer and Tachiev [20], respectively. $\lambda_{\rm NIST}$ represent the experimental NIST values by Kramida and Nave [43], and $A_{\rm Exp_{Av}}$ the weighted average experimental values.

#	Upper level (k)	Lower level (i)	$\lambda_{\rm TW}$	$\lambda_{\rm NIST}$	$A_{\rm TW,l}$	$A_{\rm TW,v}$	$A_{\rm G}$	$A_{\rm M}$	$A_{\rm BH}$	$A_{\rm FH}$	$A_{\rm GF}$	$A_{\rm Z}$	$A_{\rm FT}$	$A_{\rm Exp_{Av}}$
	$(^3P)3d-(^3P)3p$													
1	$^2P_{1/2}$	$^2S_{1/2}$	357.68	350.36	2.01	2.12	1.90	1.99	2.01	2.03	···	1.65	2.10	2.32±0.14
2	$^2D_{3/2}$	$^2P_{1/2}$	397.81	381.84	0.71	0.68	0.69	0.64	1.06	0.67	···	···	0.68	0.56±0.05
3		$^2P_{3/2}$	366.58	380.00	0.14	0.11	···	0.36	0.57	0.35	···	0.30	0.37	0.30±0.03
4	$^2D_{5/2}$	$^2P_{3/2}$	399.01	382.98	0.84	0.73	0.88	0.93	1.68	0.90	···	···	0.98	0.79±0.07
5		$^2D_{3/2}$	355.28	347.76	0.27	0.30	0.34	0.44	0.50	0.33	···	···	0.33	0.30±0.03
6		$^4D_{3/2}$	337.51	326.99	0.29	0.29	0.48	0.24	0.00	0.39	···	···	0.37	0.3±0.09
7	$^2F_{5/2}$	$^2P_{3/2}$	391.94	375.38	0.21	0.18	0.55	0.52	0.12	0.05	···	···	0.16	0.26±0.06
8		$^4D_{3/2}$	307.34	321.43	0.01	0.01	1.61	0.65	0.00	0.14	···	···	0.20	0.75±0.23
9	$^2F_{7/2}$	$^2D_{5/2}$	357.05	340.69	2.00	2.10	1.10	1.47	3.61	1.64	1.89	···	1.61	1.16±0.06
10		$^4D_{7/2}$	311.85	320.90	0.10	0.09	0.12	0.15	0.00	0.16	0.19	···	0.16	0.11±0.01
11	$^4P_{1/2}$	$^4P_{1/2}$	293.32	292.56	0.56	0.48	0.52	0.56	0.56	0.41	···	···	0.49	0.52±0.16
12		$^4P_{3/2}$	291.01	298.40	1.57	1.38	···	···	0.49	1.11	···	1.48	1.46	1.70±0.51
13		$^4S_{3/2}$	373.65	379.55	1.28	1.42	···	···	1.54	1.16	···	1.54	1.47	1.30±0.39
14	$^4P_{3/2}$	$^4S_{3/2}$	356.58	369.51	0.96	1.05	0.82	1.06	1.67	0.30	···	···	1.01	0.57±0.04
15		$^4P_{5/2}$	302.96	287.30	0.48	0.43	0.46	0.63	0.96	0.08	···	···	0.45	0.34±0.10
16		$^4D_{1/2}$	308.05	320.94	0.11	0.11	0.51	0.17	0.05	1.48	···	···	0.34	0.39±0.12
17		$^4D_{3/2}$	319.46	334.05	0.29	0.30	0.14	0.34	0.11	0.96	···	···	0.49	0.29±0.09
18	$^4P_{5/2}$	$^4S_{3/2}$	365.35	354.28	1.32	1.41	1.30	1.33	1.94	1.22	···	···	1.49	1.29±0.10
19		$^4P_{3/2}$	293.82	287.63	0.64	0.58	0.84	0.83	0.73	0.18	···	···	0.70	0.22±0.06
20		$^4P_{5/2}$	300.37	285.80	0.72	0.67	0.91	0.84	1.23	0.05	···	···	0.72	0.25±0.07
21		$^2D_{3/2}$	348.54	337.18	0.25	0.25	0.12	0.18	0.00	0.71	···	···	0.17	0.23±0.07
22		$^4D_{3/2}$	313.05	317.61	0.03	0.25	0.03	0.15	0.04	0.14	···	···	0.06	0.06±0.02
23	$^4D_{1/2}$	$^4P_{1/2}$	308.65	304.56	2.40	0.02	2.50	2.56	3.00	2.50	···	2.37	2.40	2.77±0.59
24		$^4P_{3/2}$	319.84	302.87	0.73	0.72	0.84	0.85	0.88	0.82	···	···	0.80	0.60±0.18
25		$^4D_{3/2}$	336.29	347.13	0.32	0.35	···	···	0.41	0.39	···	0.39	0.37	0.35±0.11
26		$^4D_{1/2}$	337.93	341.09	0.26	0.29	···	···	0.36	0.29	···	0.38	0.30	0.30±0.09
27	$^4D_{3/2}$	$^4P_{1/2}$	322.26	305.47	0.80	0.82	0.93	0.98	1.21	0.96	···	1.17	0.92	0.87±0.18
28		$^4P_{3/2}$	315.53	303.77	1.84	1.80	2.00	2.04	2.27	1.97	···	···	1.91	2.02±0.19
29		$^4P_{5/2}$	313.13	301.73	0.34	0.33	0.35	0.35	0.35	0.34	···	···	0.33	0.64±0.19
30		$^4D_{3/2}$	337.41	348.16	0.27	0.30	0.38	0.31	0.37	0.29	···	···	0.30	0.27±0.03
31	$^4D_{5/2}$	$^4P_{3/2}$	306.41	304.76	1.68	1.58	1.80	1.82	2.18	1.82	···	1.98	1.74	1.87±0.40
32		$^4P_{5/2}$	309.36	302.70	1.47	1.36	1.50	1.48	1.54	1.38	···	···	1.36	1.46±0.14
33		$^4D_{5/2}$	335.78	346.58	0.48	0.51	0.55	0.48	0.62	0.49	···	0.44	0.49	0.49±0.06
34	$^4D_{7/2}$	$^4P_{5/2}$	303.45	320.41	2.65	2.66	3.10	3.16	3.53	3.06	3.02	2.84	2.95	2.73±0.21
35		$^4D_{7/2}$	342.25	332.92	0.87	0.93	0.87	0.89	1.07	0.92	···	0.67	0.89	0.87±0.06
36	$^4F_{3/2}$	$^4S_{3/2}$	363.03	357.12	0.03	0.04	0.43	0.27	0.00	1.30	···	···	0.46	0.92±0.04
37		$^4D_{3/2}$	327.81	319.89	0.59	0.60	0.59	0.48	1.06	0.00	···	···	0.36	0.32±0.10
38	$^4F_{5/2}$	$^2D_{3/2}$	326.88	338.84	0.02	0.02	2.00	1.64	0.00	0.09	···	···	0.08	1.53±0.33
39		$^4D_{3/2}$	331.33	321.43	1.94	2.06	0.73	0.86	3.39	2.38	···	···	2.31	0.94±0.28
40	$^4F_{7/2}$	$^2D_{5/2}$	354.17	336.72	1.37	1.41	1.00	1.43	0.00	1.60	1.79	···	1.60	1.23±0.09
41		$^4D_{5/2}$	318.50	319.86	1.69	1.40	2.30	1.87	3.86	1.66	1.49	···	1.61	0.98±0.08
42	$^4F_{9/2}$	$^4D_{7/2}$	328.89	321.82	3.52	3.58	3.60	3.70	4.23	3.73	···	3.45	3.65	3.66±0.63

Table 4. Relative differences $R_{\rm TW}$, $R_{\rm TW,adjusted}$, and $R_{\rm FT}$ between the theoretical transition probability values $A_{\rm TW,l}$, $A_{\rm TW,l\ adjusted}$, and $A_{\rm FT}$, and the $A_{\rm Exp_{Av}}$ weighted average experimental values, respectively.

#	Upper level (k)	Lower level (i)	$R_{\rm TW}$	$R_{\rm TW,adjusted}$	$R_{\rm FT}$
	$(^3P)3p - (^3P)3s$				
5	$^2P_{3/2}$	$^2P_{1/2}$	-10 %	2 %	-2 %
18	$^4P_{5/2}$	$^4P_{3/2}$	-13 %	-3 %	-10 %
	$(^1D)3p - (^1D)3s$				
29	$^2P_{3/2}$	$^2D_{3/2}$	-24 %	-13 %	-26 %

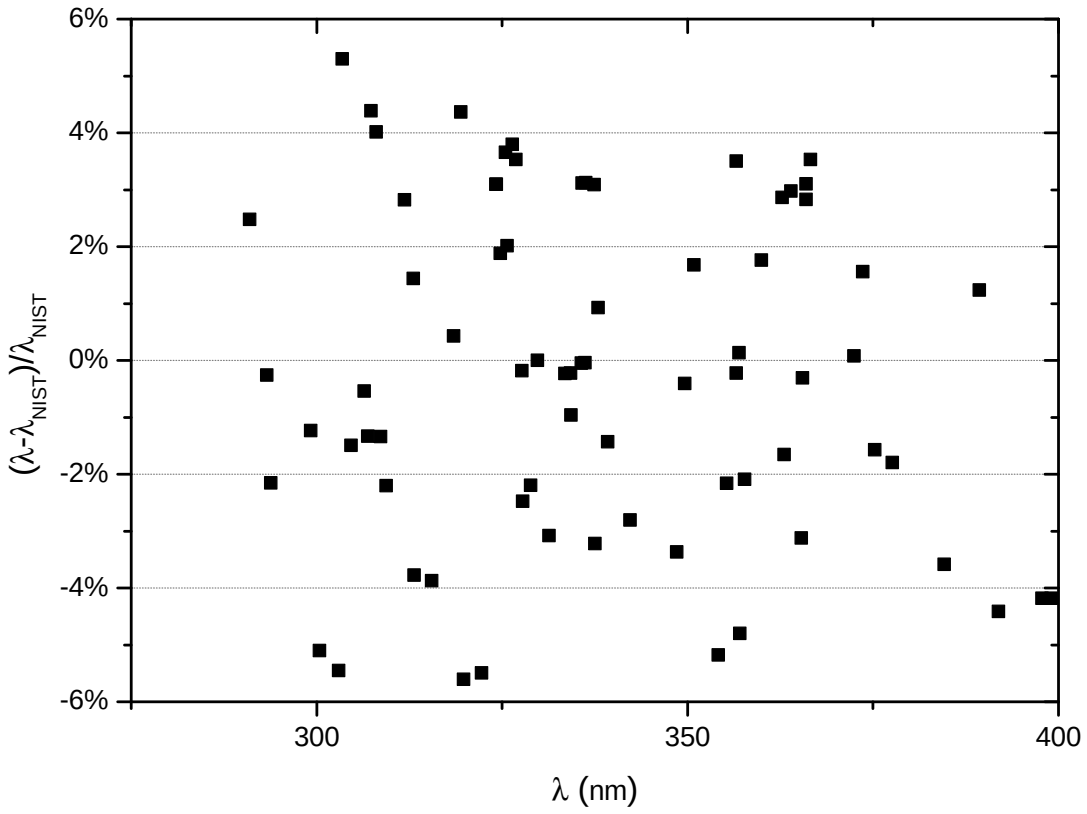

Fig. 1. Relative difference between the theoretical wavelengths calculated in this work and the experimental results by Kramida and Nave [43].

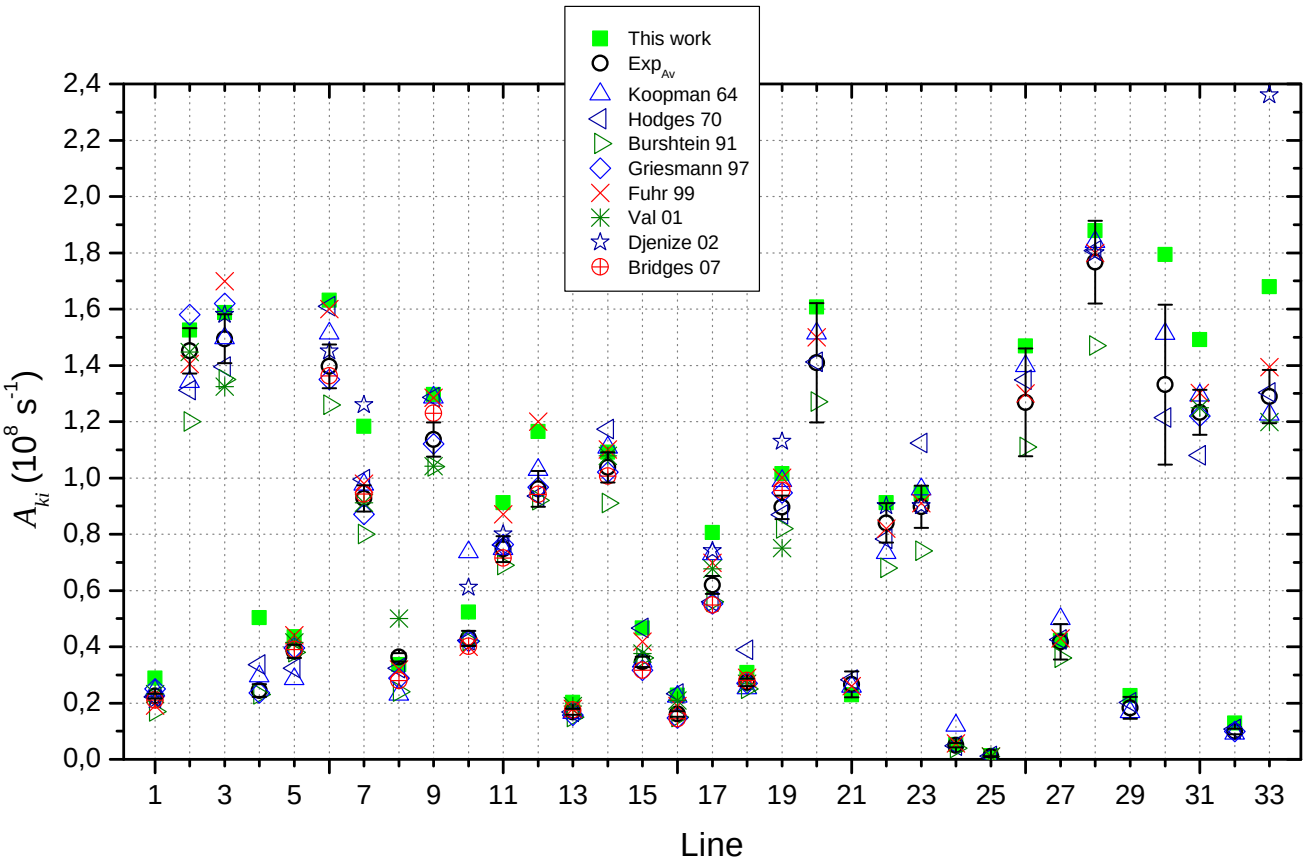

Fig. 2. Comparison of our theoretical results and the available experimental results for $3p - 3s$ transition probability values.

4 Conclusions

We presented *ab initio* relativistic calculated values of transition wavelengths and probabilities for several $2p^4$ 3p - $2p^4$ 3s and $2p^4$ 3d - $2p^4$ 3p lines Ne II. These transitions are of interest because of their importance in the interpretation of stellar thermonuclear reactions. We showed the importance of the inclusion of correlation in a balanced way. The results are compared with existing theoretical calculations and with experimental data. The dispersion of experimental results for each analyzed transition prevents the assessment of the available theoretical data, calling for more accurate experimental results.

Acknowledgments

This research was supported in part by FCT (Portugal), by the French-Portuguese Collaboration (PESSOA Hubert Curien Program, Contract Nº 10721NF and 20022VB), and by the Acções Integradas Luso-Francesas (Contract Nº F-11/09). Laboratoire Kastler Brossel (LKB) is "Unité Mixte de Recherche du CNRS, de l'ENS et de l'UPMC N° 8552". The LKB group acknowledges the support of the Allianz Program of the Helmholtz Association, contract EMMI HA-216 "Extremes of Density and Temperature: Cosmic Matter in the Laboratory".

References

1. D. E. Osterbrock, *Astrophysics of Gaseous Nebulae and Active Galactic Nuclei* (University of Science, Mill Valley, CA, 1989).
2. V. Trimble, Astronomy and Astrophysics Review **3**, 1 (1991).
3. D. W. Koopman, J. Opt. Soc. Am. A **54**, 1354 (1964).
4. E. R. Condon G. H. Shortley, *The Theory of Atomic Spectra* (Cambridge University Press, Cambridge, 1953).
5. NIST Atomic Spectra Database v3.0, http://physics.nist.gov/PhysRefData/ASD/index.html, 2008.
6. D. Hodges, H. Marantz, C. L. Tang, J. Opt. Soc. Am. A **60**, 192 (1970).
7. M. L. Burshtein V. Vujnovic, Astron. Astrophys. **247**, 252 (1991).
8. U. Griesmann, J. Musielok, W. L. Wiese, J. Opt. Soc. Am. B **14**, 2204 (1997).
9. J. R. Fuhr W. L. Wiese, *CRC Handbook of Chemistry and Physics* (CRC Press, Boca Raton, Florida, 1999), pp. 10–88.
10. J. A. del Val, J. A. Aparicio, V. R. Gonzalez, S. Mar, J. Phys. B **34**, 2513 (2001).
11. S. Djenize, V. Milosavljevic, M. S. Dimitrijevic, Astron. Astrophys. **382**, 359 (2002).
12. J. M. Bridges W. L. Wiese, Phys. Rev. A **76**, 022513 (2007).
13. R. H. Garstang, Mon. Not. R. Astron. Soc. **114**, 118 (1954).
14. H. Marantz, Ph.D. thesis, Cornell University, 1968, published in [6].
15. F. Herman S. Skillman, *Atomic Structure Calculations* (Prentice Hall, USA, 1963).
16. H. M. S. Blackford A. Hibbert, At. Data Nucl. Data Tables **58**, 101 (1994).
17. C. Froese Fischer X. He, Can. J. Phys. **77**, 177 (1999).
18. M. R. Godefroid A. Hibbert, Mol. Phys. **98**, 1099 (2000).
19. N. W. Zheng T. Wang, Spectrochim. Acta Part B **58**, 1319 (2003).
20. C. Froese Fischer G. Tachiev, At. Data Nucl. Data Tables **87**, 1 (2004).
21. J. P. Desclaux, Comp. Phys. Commun. **9**, 31 (1975).
22. P. Indelicato, Phys. Rev. Lett. **77**, 3323 (1996).
23. P. Indelicato J. Desclaux, MCDFGME, a MultiConfiguration Dirac Fock and General Matrix Elements program (release 2005), `http://dirac.spectro.jussieu.fr/mcdf`, 2007.
24. P. Indelicato, Phys. Rev. A **51**, 1132 (1995).
25. G. E. Brown D. E. Ravenhall, Proc. R. Soc. London, Ser. A **208**, 552 (1951).
26. J. Sucher, Phys. Rev. A **22**, 348 (1980).
27. M. H. Mittleman, Phys. Rev. A **24**, 1167 (1981).
28. O. Gorceix P. Indelicato, Phys. Rev. A **37**, 1087 (1988).
29. G. Audi, A. H. Wapstra, C. Thibault, Nucl. Phys. A **729**, 337 (2003).
30. I. Angeli, At. Data Nucl. Data Tables **87**, 185 (2004).
31. P. J. Mohr Y.-K. Kim, Phys. Rev. A **45**, 2727 (1992).
32. P. J. Mohr, Phys. Rev. A **46**, 4421 (1992).
33. E.-O. Le Bigot, P. Indelicato, P. J. Mohr, Phys. Rev. A **64**, 052508 (2001).
34. P. Indelicato P. Mohr, Phys. Rev. A **46**, 172 (1992).
35. P. J. Mohr G. Soff, Phys. Rev. Lett. **70**, 158 (1993).
36. P. Indelicato, O. Gorceix, J. P. Desclaux, Journal of Physics B: Atomic and Molecular Physics **20**, 651 (1987).
37. P. Indelicato J. P. Desclaux, Phys. Rev. A **42**, 5139 (1990).
38. P. Indelicato E. Lindroth, Phys. Rev. A **46**, 2426 (1992).
39. P. Indelicato, S. Boucard, E. Lindroth, Eur. Phys. J. D **3**, 29 (1998).
40. P. Indelicato P. Mohr, Hyp. Int. **114**, 147 (1998).
41. P. Indelicato, Hyp. Int. **108**, 39 (1997).
42. P.-O. Lowdin, Phys. Rev. **97**, 1474 (1955).
43. A. E. Kramida G. Nave, Eur. Phys. J. D **39**, 331 (2006).
44. P. Indelicato, E. Lindroth, J. P. Desclaux, Phys. Rev. Lett. **94**, 013002 (2005).
45. A. I. Akhiezer V. B. Berestetskii, *Quantum Electrodynamics*, *Interscience Monographs and Texts in Physics and Astronomy* (Interscience Publishers, New York, 1965).
46. I. P. Grant, Journal of Physics B: Atomic and Molecular Physics **7**, 1458 (1974).
47. U. I. Safronova, W. R. Johnson, A. E. Livingston, Phys. Rev. A **60**, 996 (1999).
48. A. F. Starace, Phys. Rev. A **3**, 1242 (1971).
49. A. F. Starace, Phys. Rev. A **8**, 1141 (1971).
50. A. Derevianko, I. M. Savukov, W. R. Johnson, D. R. Plante, Phys. Rev. A **58**, 4453 (1998).

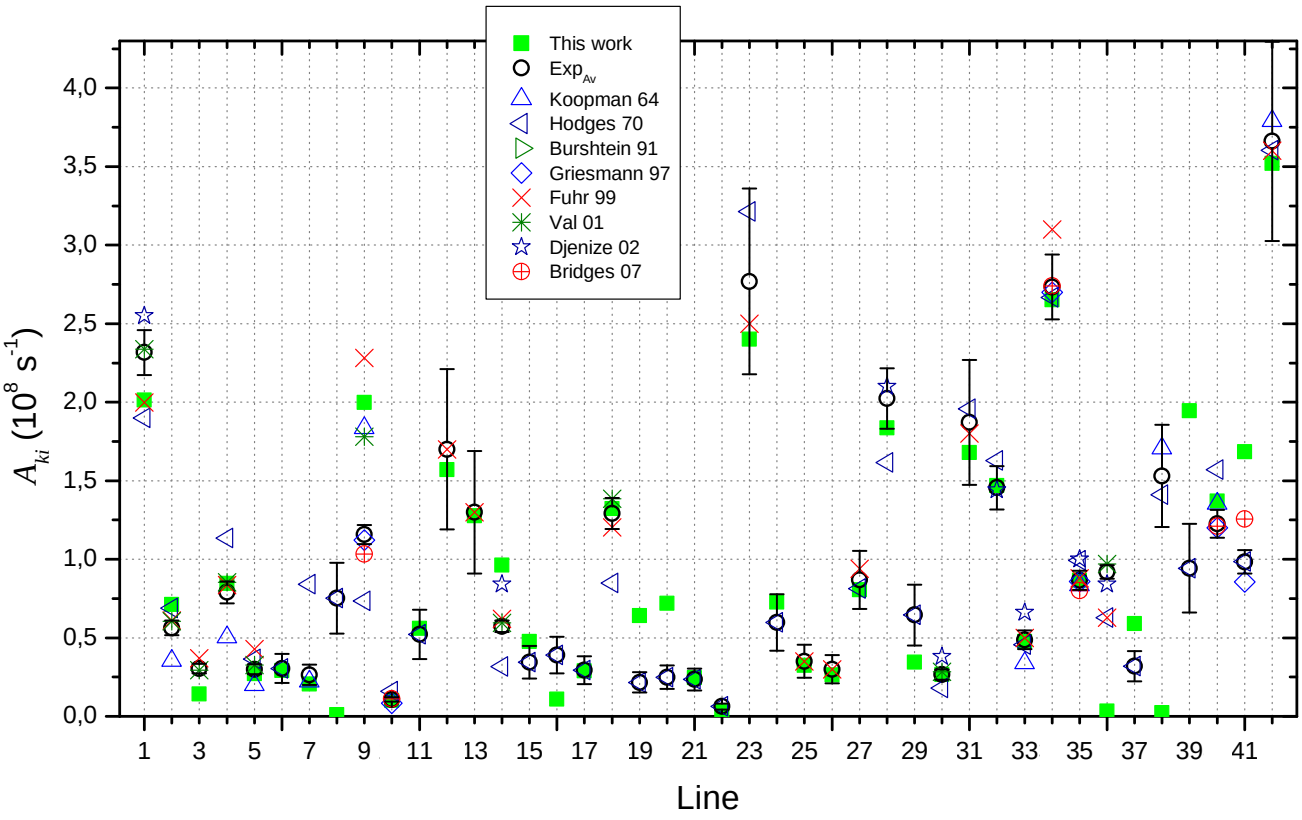

Fig. 3. Comparison of our theoretical results and the available experimental results for $3d - 3p$ transition probability values.